



**HAL**  
open science

# Exploring Control Co-Design's Versatility in System Optimisation: A Case Study of DC Motors

Thalita Nazaré, Isabelle Queinnec, Erivelton Nepomuceno

## ► To cite this version:

Thalita Nazaré, Isabelle Queinnec, Erivelton Nepomuceno. Exploring Control Co-Design's Versatility in System Optimisation: A Case Study of DC Motors. 32nd Mediterranean Conference on Control and Automation (MED 2024), IEEE, Jun 2024, Chania, Crete, Greece. 10.1109/MED61351.2024.10566157 . hal-04654734

**HAL Id: hal-04654734**

**<https://laas.hal.science/hal-04654734v1>**

Submitted on 19 Jul 2024

**HAL** is a multi-disciplinary open access archive for the deposit and dissemination of scientific research documents, whether they are published or not. The documents may come from teaching and research institutions in France or abroad, or from public or private research centers.

L'archive ouverte pluridisciplinaire **HAL**, est destinée au dépôt et à la diffusion de documents scientifiques de niveau recherche, publiés ou non, émanant des établissements d'enseignement et de recherche français ou étrangers, des laboratoires publics ou privés.

# Exploring Control Co-Design's Versatility in System Optimisation: A Case Study of DC Motors

Thalita Nazaré  
Centre for Ocean Energy Research  
Department of Electronic Engineering  
Maynooth University  
Maynooth, Ireland  
thalita.nazare.2023@mumail.ie

Isabelle Queinnec  
LAAS-CNRS  
Université de Toulouse, CNRS  
Toulouse, France  
isabelle.queinnec@laas.fr

Erivelton Nepomuceno  
Centre for Ocean Energy Research  
Department of Electronic Engineering  
Maynooth University  
Maynooth, Ireland  
erivelton.nepomuceno@mu.ie

**Abstract**—This study explores the integration of Control Co-Design (CCD) with Linear Quadratic Regulator (LQR) optimisation to enhance DC motor performance. Focusing on early design stages, it demonstrates how CCD and LQR can cooperatively improve system parameters, addressing both step and triangular disturbances. Results show significant enhancements, including up to 44.3% overshoot reduction and 62.2% energy consumption decrease, alongside a notable reduction in maximum actuator voltage by 51.1%. These findings underscore the technical advantages of incorporating CCD and LQR optimisation from the outset of system design, offering a comprehensive framework for achieving superior system performance, adaptability, and efficiency. The results contribute valuable technical insights into the application of CCD in system optimisation.

**Index Terms**—Control Co-design, optimisation, LQR control, DC motor.

## I. INTRODUCTION

Optimisation in engineering, a concept of paramount importance, finds relevance in a wide range of disciplines, significantly contributing to advances in system performance and efficiency [1, 2]. Its strategic application spans diverse fields, from refining flight trajectories in aerospace engineering [3] to enhancing power distribution in electrical systems [4]. The importance of optimisation is not restricted to intricate or extensive systems; its pertinence extends to apparently simpler systems, where even minor enhancements might result in substantial benefits. Examples include mechanical systems like pulleys and gears, whose efficiency can directly impact manufacturing processes, or basic electrical circuits, where optimisation can lead to energy savings and improved performance [5, 6].

Although optimisation is widely used, there is a tendency, especially in control systems, to delay the implementation of optimisation tactics until later phases of development [7]. The literature examines this subject in many settings, but there is still need for a more targeted investigation into the integration of early-stage optimisation. This is particularly important given the potential benefits that such integration may have on the efficiency and effectiveness of systems.

This work was supported by Maynooth University via a John and Pat Hume Doctoral (WISH) for Thalita Nazaré and Erivelton Nepomuceno, under Grant number 21/FFP-P/10065.

Addressing this gap, Control Co-Design emerges as a transformative approach, integrating control strategies right from the initial design stages [8]. This methodology is a departure from conventional design processes, where control aspects are considered post-facto [9]. However, control co-design is more applied in systems with high dynamic coupling, as it is not common to encounter applicability in non-complex systems in the literature. Therefore, some examples of CCD applied to systems with high dynamic complexity include satellites [10], control of vehicular platoons [11, 12], vehicular suspension [13], robotics [14, 15], redundant actuation [16] and aircraft [17].

On the other hand, the holistic approach of CCD could also be advantageous for simpler systems, where traditional approaches may neglect the potential gains from early-stage optimisation. In simpler systems, applying CCD can lead to design solutions that are not only efficient but also cost-effective. The early integration of control strategies can simplify the system architecture, reducing the need for complex and expensive hardware, thereby lowering production costs and simplifying maintenance and operation. Furthermore, CCD in simpler systems can enhance modularity, allowing for easy upgrades and scalability, which is crucial for adapting to evolving academic research and experimental needs.

In this work, the application of CCD, coupled with optimisation techniques, is explored through the optimisation of a DC motor. Despite being a fundamental and seemingly straightforward component in many engineering applications, ranging from small consumer devices to larger industrial machines [18, 19], the DC motor exemplifies a system where CCD can significantly enhance performance. By embedding advanced control strategies, such as the Linear Quadratic Regulator, into the motor's design phase, the study aims to demonstrate the efficacy of CCD in optimising even the simpler systems. This analysis is critical in assessing the effectiveness of each strategy in refining the LQR parameters and understanding their impacts on the performance of the DC motor. Through this exploration, the research offers insights into the application of these techniques in enhancing simpler engineering systems.

## II. CONTROL CO-DESIGN OVERVIEW

Control co-design, which integrates control principles from the start, is a novel approach to system design and development. According to [8], this paradigm shift prioritises simultaneous consideration of control systems and physical components during design, unlike traditional practices that move control to a later stage. CCD involves the system control team from the start to achieve synergistic system optimisation rather than subsystem optimisation. Integration may increase control efficiency, cost reduction, and product dependability [20].

According to Garcia-Sanz [8], CCD is usually delimited by co-optimisation, co-simulation, and control-inspired paradigms. Co-optimisation involves optimising both the control system and the physical system simultaneously, rather than optimising them separately as in traditional design processes [21]. This approach can lead to improved system performance and reduced design time. Co-simulation is another technique that involves simulating both the control system and the physical system together, allowing engineers to test and optimise the system as a whole [22]. This approach can help identify potential issues and improve system performance. Control-inspired design, as the name suggests, involves drawing inspiration from control theory to design other engineering systems [23]. For example, engineers may use the principles of feedback control to design systems that can adapt and self-correct in response to changing conditions.

The CCD approach can be summarised by three model-based strategies: iterative, simultaneous, and nested [24]. In this article it was applied the simultaneous strategy that integrates all dynamic system-control interactions within a single optimisation model, thus ensuring a comprehensive and system-level optimal outcome. This method facilitates the concurrent optimisation of both system and control variables, which enhances the efficiency and effectiveness through bidirectional coupling, as follows the optimisation formulation with two sets of disciplinary design variables,  $\mathbf{x}$  and  $\mathbf{y}$ , and three sets of constraints,  $g_x(\mathbf{x})$ ,  $g_y(\mathbf{y})$ , and  $g_{xy}(\mathbf{x}, \mathbf{y})$ .

$$\begin{aligned} & \min f(\mathbf{x}) + f(\mathbf{y}) + f(\mathbf{x}, \mathbf{y}) \\ & \text{subject to } g_x(\mathbf{x}) \leq 0, \quad g_y(\mathbf{y}) \leq 0 \\ & \quad \quad \quad g_{xy}(\mathbf{x}, \mathbf{y}) \leq 0 \end{aligned}$$

## III. FORMULATION OF THE CO-DESIGN AND OPTIMISATION PROBLEM

This section discusses the optimisation of DC motor control parameters. This optimisation challenge involves modifying DC motor and control settings to achieve control goals and improve performance. Optimising motor performance within restrictions is often the main focus. The settings are adjusted to minimise a stated objective function, which measures system performance. This optimisation method uses control co-design, which considers the system model and control design concurrently. Optimising motor characteristics and control technique together improves system performance.

### A. Control Formulation

The DC motor design in Fig. 1 includes key features including armature resistance ( $R$ ), armature inductance ( $L$ ), and the back electromotive force ( $V_{emf}$ ), which is the voltage caused by the changing magnetic field.

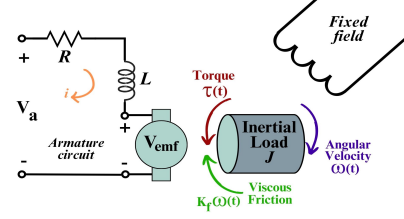


Fig. 1: The structure of the DC motor.

The motor's transfer function is modelled by the following equation:

$$\frac{\omega(s)}{V_a(s)} = \frac{K_m}{(Ls + R)(Js + K_f) + K_m K_b}. \quad (1)$$

The block diagram presented in Fig. 2 denotes a LQR control system employed to regulate the speed of the DC motor. This specific implementation includes an integration of the error signal, which suggests the incorporation of an integral action in the control scheme to eliminate steady-state errors, enhancing the system's response to disturbances.

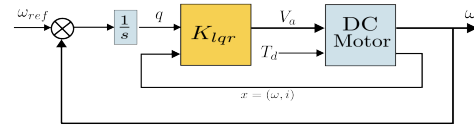


Fig. 2: Design of the linear quadratic regulator for the feedback structure.

Based on the Newton's law combined with the Kirchoff's law, the state vector for the system is defined as  $x = (\omega, i)$  where  $i$  represents the armature current and  $\omega$  represents the motor speed. The LQR technique utilises the state vector  $x$  along with the integral of error to generate the driving voltage  $V_a$ . The resultant voltage assumes the form of:

$$V_a = K_1 \times \omega + K_2 \times \frac{\omega}{s} + K_3 \times i, \quad (2)$$

where  $[K_1 \ K_2 \ K_3]$  are the controller's gains. The control objective is to manipulate the driving voltage,  $V_a$ , based on the state feedback and the error integral, to ensure that  $\omega$  tracks the reference speed,  $\omega_{ref}$ , as closely as possible. To synthesise the control signal, a cost function is employed which penalises large integral errors for  $Q_{22} \gg 1$ :

$$J_{lqr} = \int_{t_0}^{t_1} (Q_{22}q(t)^2 + Q_{11}\omega(t)^2 + R_{lqr}V_a(t)^2) dt, \quad (3)$$

$$\text{where } q(s) = \frac{\omega(s)}{s}, \quad Q_{lqr} = \begin{bmatrix} Q_{11} & 0 \\ 0 & Q_{22} \end{bmatrix}.$$

This is indicative of a weighted approach within the cost function where the integral of the error, signifying the accumulated discrepancy over time between the desired and actual output, is given considerable significance. By imposing a heavier penalty on the integral of the error, the LQR controller is tuned to be more sensitive to the sustained errors, thereby reinforcing the system's robustness against disturbances and model uncertainties.

The enhanced system's dynamics, utilising the motor model and integral action to represent speed, compute the LQR gain,  $K_{lqr}$ . Including the error integral in state-space requires this adjustment. Creating a compensator after calculating LQR gain completes the plant's open-loop system. Open-loop systems are regulated by feedback operations that compare output and input. Complete status feedback is provided to the controller for all system states. This creates the closed-loop system and retrieves the transfer function that relates the reference speed, disturbances, and output speed for simulation.

### B. Optimisation Problem Formulation

The generic formulation of a simultaneous optimisation problem for DC motor control can be expressed as:

$$\begin{aligned} &\min f(\mathbf{x}) + f(\mathbf{y}) + f(\mathbf{x}, \mathbf{y}) \\ &\text{subject to } g_x(\mathbf{x}) \leq 0, \quad g_y(\mathbf{y}) \leq 0 \\ &\quad g_{xy}(\mathbf{x}, \mathbf{y}) \leq 0 \\ &\quad \mathbf{x}_{\min} \leq \mathbf{x} \leq \mathbf{x}_{\max} \\ &\quad \mathbf{y}_{\min} \leq \mathbf{y} \leq \mathbf{y}_{\max} \end{aligned}$$

- $f(\mathbf{x})$  and  $f(\mathbf{y})$  represent the functions that assess the performance of the DC motor, specifically measuring the overshoot and energy consumption. These functions are intricately linked to the employed control strategy.
- The simultaneous optimisation of the function  $f(\mathbf{x}, \mathbf{y})$  is achieved by assigning complementary weights to the metrics, as delineated in Eq. 5. This allocation ensures that the sum of the weights equals 1, thereby facilitating a balanced consideration of the trade-offs between overshoot and energy consumption. This approach guarantees that enhancements in one metric do not detrimentally impact the other.
- $\mathbf{x}$  and  $\mathbf{y}$  are the vectors of decision variables corresponding to the DC motor parameters  $R$ ,  $L$ ,  $K_m$ ,  $K_b$ ,  $K_f$ ,  $J$ , and in the case of LQR,  $Q_{11}$ ,  $Q_{22}$ , and  $R_{lqr}$ .

By the armature voltage,  $V_a$  calculated in Eq.(2) and the armature current,  $i$  (one of system states), it is possible to calculate the power ( $P_a$ ) and, consequently, the energy consumed. This energy is one of the metrics aimed to be minimised in the cost function.

$$\text{Energy} = \int_0^t P_a(t) dt \quad (4)$$

The objective function,  $f(\mathbf{x})$ , expresses DC motor performance measures. The goal function is a linear mixture of normalised performance measurements.

$$\text{cost} = \lambda \times \text{Overshoot} + \phi \times \text{Energy}, \quad (5)$$

where  $\lambda$  and  $\phi$  are the weights of each metric. This cost function evaluates control quality and balances overshoot and energy consumption to provide exact performance and energy efficiency. Overshoot and energy consumption are cost function elements for stability, user experience, mechanical stress reduction, environmental impact reduction, cost savings, and DC motor control system efficiency. A comprehensive control co-design technique highlights the connection between control strategy and system attributes for optimal performance. The optimisation procedure considers Objective Function Tolerance (fmincon function), terminating when the change in objective function value between iterations is  $\geq 10^{-6}$ . The flowchart in Fig. 3 outlines the procedures for co-design and optimisation.

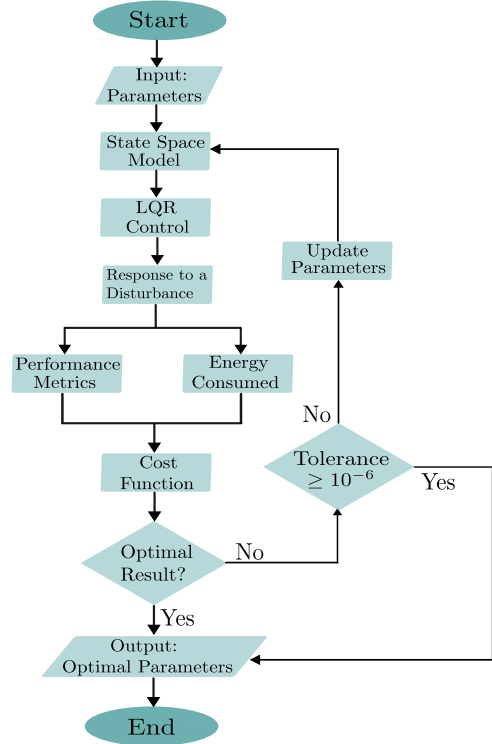


Fig. 3: Flowchart illustrating the step-by-step methodology.

### IV. NUMERICAL EXAMPLE

The adaptability and efficiency of the CCD technique in optimising the performance of a DC motor control system is shown by its application in two distinct disturbances: step and ramp. By modifying the weights in the cost function to emphasise various elements of system performance, the CCD technique consistently produces satisfying outcomes that are customised to the particular disturbance being targeted.

- Case 01:  $\lambda = 0.9$  and  $\phi = 0.1$
- Case 02:  $\lambda = 0.5$  and  $\phi = 0.5$
- Case 03:  $\lambda = 0.1$  and  $\phi = 0.9$

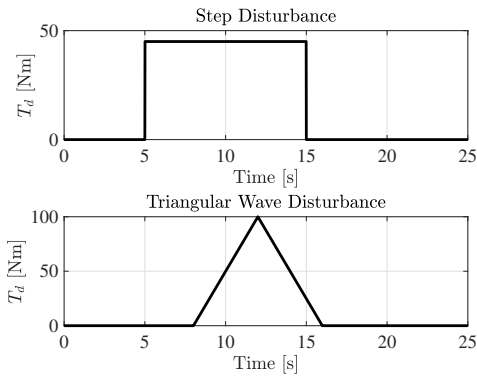


Fig. 4: The two case of disturbances.

In the present example, the parameter values for the motor were derived from the data presented in [25], where the maximum value for  $V_a$  is 280V. While respecting a parameter variation limit of 20%. Figures 5, 6, 8 and 9 illustrates the effect on the motor's performance by showing the system's temporal response for three distinct scenarios. For this example, cost function metrics were normalised to values between 0 and 1 to maintain the same influence on the weighting. The optimisation led to parameter adjustments in motors and controllers, achieving a balance between reducing overshoot and improving energy efficiency through CCD. This approach enhanced system performance, efficiency, and safety.

Furthermore, the initial parameter values significantly impact the convergence process, as indicated by the function count. For both disturbances, the count was around 100 when the initial parameters favoured overshoot reduction. However, when the weight on energy efficiency increased, the count reached nearly 300, as present in Figures (7) and (10). This emphasises the significance of initial parameters in optimisation, demonstrating that starting values closer to the aim of reducing overshoot result in more efficient convergence when the main objective is to minimise this metric. Results details follow.

### A. Step Disturbance

TABLE I: Results for step disturbance: Comparison of results with initial parameter values vs. optimised values.

	Initial Parameters	Case 01	Case 02	Case 03
$R$	0.5	0.4	0.474	0.6
$L$	0.01	0.008	0.008	0.008
$K_m$	1.23	1.476	1.476	1.024
$K_b$	1.23	1.476	1.476	1.398
$K_f$	0.02	0.024	0.024	0.019
$J$	0.05	0.06	0.041	0.04
$Q_{11}$	0.5	0.6	0.4	0.4
$Q_{22}$	10	12	10	9.99
$R_{lqr}$	0.5	0.4	0.6	0.6
<b>Metrics</b>				
<b>Energy</b>	0.119	0.139	0.059	0.045
<b>Overshoot</b>	0.181	0.120	0.147	0.203
$\max(V_a)$	265.0	253.7	159.9	129.7

For Case 01, with a weight configuration of  $\lambda = 0.9$  and  $\phi = 0.1$ , the overshoot was reduced from 0.181 to 0.120, indicating an enhancement in system response. However, this was achieved at the expense of increased energy consumption, which rose from 0.119 to 0.139. Furthermore, the maximum actuator voltage saw a reduction from 265V to 253.7V.

Case 02, where weights were balanced between overshoot and energy consumption ( $\lambda = 0.5$  and  $\phi = 0.5$ ), presented an optimal trade-off. The overshoot was moderately adjusted to 0.147, while energy consumption saw a significant decrease to 0.059. The maximum actuator voltage was notably reduced to 159.9V.

In Case 03, with a focus on energy efficiency ( $\lambda = 0.1$  and  $\phi = 0.9$ ), the lowest energy consumption was achieved at 0.045, albeit with an increase in overshoot to 0.203. This scenario also saw the most substantial reduction in maximum actuator voltage to 129.7V. The increase in resistance to 0.6 in this case suggests an adjustment aimed at managing energy consumption more effectively.

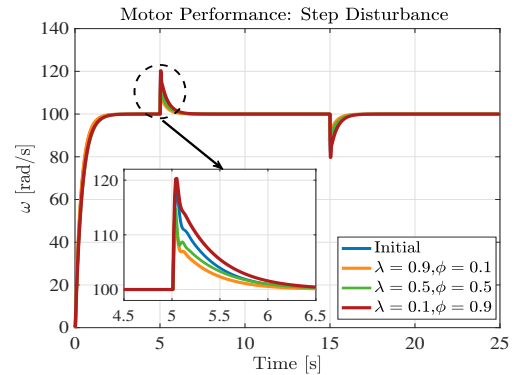


Fig. 5: Motor performance was assessed by comparing results for the initial values with the results under step disturbance.

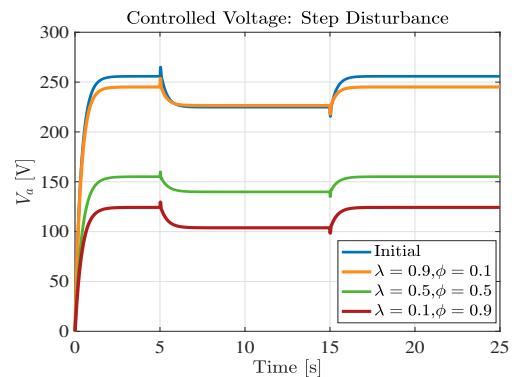


Fig. 6: Controlled voltage performance for three distinct scenarios of optimisation under step disturbance.

### B. Triangular Wave Disturbance

In Case 01, the emphasis on minimising overshoot led to a reduction from the initial 0.309 to 0.172. This improvement in system response was slightly offset by a marginal increase

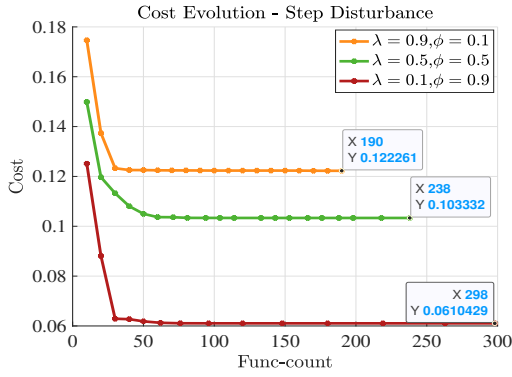


Fig. 7: Cost evaluation for the optimisation cases under step disturbance.

TABLE II: Results for triangular wave disturbance: Comparison of results with initial parameter values vs. optimised values.

	Initial Parameters	Case 01	Case 02	Case 03
$R$	0.5	0.4	0.4	0.557
$L$	0.01	0.008	0.008	0.008
$K_m$	1.23	1.476	1.476	1.476
$K_b$	1.23	1.476	1.476	1.476
$K_f$	0.02	0.024	0.024	0.024
$J$	0.05	0.06	0.04	0.04
$Q_{11}$	0.5	0.4	0.4	0.4
$Q_{22}$	10	12	12	12
$R_{lqr}$	0.5	0.4	0.4	0.6
<b>Metrics</b>				
<b>Energy</b>	0.120	0.122	0.074	0.055
<b>Overshoot</b>	0.309	0.172	0.188	0.259
$\max(V_a)$	256.0	213.2	196.6	146.4

in energy consumption from 0.120 to 0.122. Furthermore, the maximum actuator voltage was reduced from 256V to 213.2V.

Case 02 balanced the weights for overshoot and energy consumption, achieving a compromise with the overshoot adjusted to 0.188 and a notable reduction in energy consumption to 0.074. The maximum actuator voltage witnessed a further reduction to 196.6V.

In Case 03, the lowest energy consumption was recorded at 0.055, albeit at the cost of increased overshoot to 0.259. This scenario also saw the most substantial reduction in maximum actuator voltage to 146.4V. As in the first disturbance, the increase in resistance to 0.557 suggests an adjustment aimed at managing energy consumption more effectively.

## V. CONCLUSION

In this study, the integration of CCD in the early stages of DC motor system design has yielded noteworthy results, underscoring the methodology's efficacy. The research, while preliminary, demonstrates the potential benefits of incorporating CCD in the early stages of design, particularly in improving efficiency and performance. Traditionally, optimisation strategies are applied in later stages, often leading to suboptimal performance in simpler systems. This work demonstrates

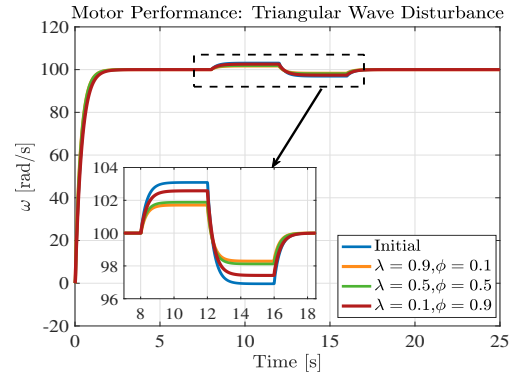


Fig. 8: Motor performance was assessed by comparing results for the initial values with the results under triangular wave disturbance.

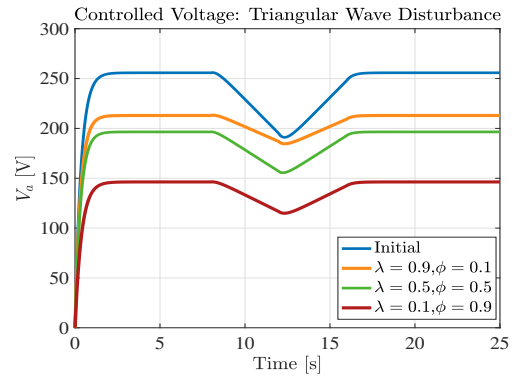


Fig. 9: Controlled voltage performance for three distinct scenarios of optimisation under triangular wave disturbance.

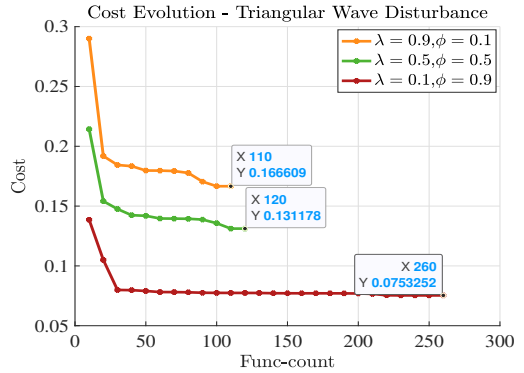


Fig. 10: Cost evaluation for the optimisation cases under triangular wave disturbance.

the substantial benefits of early-stage optimisation, particularly in terms of efficiency, reliability, and adaptability.

Applying CCD techniques on a DC motor to tackle both step and triangular disturbances revealed the approach's capability to enhance system performance through meticulous parameter adjustments. The application of CCD led to notable achievements, including overshoot reduction by up to 44.3% and energy consumption decrease by up to 62.2%, showcasing the



methodology's capability to significantly enhance operational efficiency. Additionally, the reduction in maximum actuator voltage by as much as 51.1% highlights CCD's role in improving system safety and longevity. This research underscores the importance of integrating CCD from the outset, promoting a more adaptable, efficient, and safer system design approach, and marks a significant advancement in system optimisation techniques, advocating for its early incorporation.

#### REFERENCES

- [1] T. Kipouros, D. Jaeggi, W. Dawes, G. Parks, A. M. Savill, and P. Clarkson, "Biobjective design optimization for axial compressors using tabu search," *AIAA Journal*, vol. 46, pp. 701–711, 2008.
- [2] A. Simonetto, E. Dall'Anese, S. Paternain, G. Leus, and G. Giannakis, "Time-varying convex optimization: Time-structured algorithms and applications," *Proceedings of the IEEE*, vol. 108, pp. 2032–2048, 2020.
- [3] J. Mieloszyk, A. Tarnowski, A. Tomaszewski, and T. Goetzendorf-Grabowski, "Validation of flight dynamic stability optimization constraints with flight tests," *Aerospace Science and Technology*, vol. 106, p. 106193, 2020.
- [4] T. Khurshaid, A. Wadood, S. G. Frakoush, T.-H. Kim, K.-C. Kim, and S. Rhee, "Optimal allocation of directional relay for efficient energy optimization in a radial distribution system," *Energies*, 2022.
- [5] N. W. Z. Abidin, M. Rashid, and N. Mohamed, "A review of multi-holes drilling path optimization using soft computing approaches," *Archives of Computational Methods in Engineering*, vol. 26, pp. 107–118, 2019.
- [6] G. Lin, Y. Yang, F. Pan, S. Zhang, F.-H. Wang, and S. Fan, "An optimal energy-saving strategy for home energy management systems with bounded customer rationality," *Future Internet*, vol. 11, p. 88, 2019.
- [7] P. B. Betoret, I. Ripoll, J. V. Canet, and A. Crespo, "A task model to reduce control delays," *Real-Time Systems*, vol. 27, pp. 215–236, 2004.
- [8] M. Garcia-Sanz, "Control co-design: An engineering game changer," *Advanced Control for Applications: Engineering and Industrial Systems*, vol. 1, 2019.
- [9] P. Albertos, A. Crespo, J. Simó, and A. Fernández, "Control co-design: Algorithms and their implementation," in *Reliable Software Technology - Ada-Europe 2010* (J. Real and T. Vardanega, eds.), vol. 6106 of *Lecture Notes in Computer Science*, pp. 12–26, Springer, 2010.
- [10] C. Toglia, P. Pavia, G. Campolo, D. Alazard, T. Loquen, H. de Plinval, C. Cumer, M. Casasco, and L. Massotti, "Optimal co-design for earth observation satellites with flexible appendages," *AIAA Guidance, Navigation, and Control (GNC) Conference*, pp. 1–14, 2013.
- [11] T. Zeng, O. Semiari, W. Saad, and M. Bennis, "Integrated Communications and Control Co-Design for Wireless Vehicular Platoon Systems," in *IEEE International Conference on Communications*, vol. 2018-May, Institute of Electrical and Electronics Engineers Inc., jul 2018.
- [12] Y. Hu, C. Chen, J. He, and B. Yang, "Prediction-based Transmission-Control Codesign for Vehicle Platooning," in *IEEE Vehicular Technology Conference*, vol. 2020-Novem, Institute of Electrical and Electronics Engineers Inc., nov 2020.
- [13] I. Ahmad, X. Ge, and Q. L. Han, "Communication-Constrained Active Suspension Control for Networked In-Wheel Motor-Driven Electric Vehicles with Dynamic Dampers," *IEEE Transactions on Intelligent Vehicles*, vol. 7, pp. 590–602, sep 2022.
- [14] K. Wu and G. Zheng, "Simulation and control co-design methodology for soft robotics; simulation and control co-design methodology for soft robotics," in *2020 39th Chinese Control Conference (CCC)*, 2020.
- [15] G. Fadini, T. Flayols, A. Del Prete, N. Mansard, and P. Souères, "Computational design of energy-efficient legged robots: Optimizing for size and actuators," in *2021 IEEE International Conference on Robotics and Automation (ICRA)*, pp. 9898–9904, 2021.
- [16] G. Grandesso, G. Bravo-Palacios, P. M. Wensing, M. Fontana, and A. D. Prete, "Exploring the limits of a redundant actuation system through co-design," *IEEE Access*, vol. 9, pp. 56802–56811, 2021.
- [17] M. D. Ilić and R. Jaddivada, "Making flying microgrids work in future aircrafts and aerospace vehicles," jan 2021.
- [18] L. Wei-dong, "On dc generator principle,armature reaction and commutation," *Enterprise Science and Technology & Development*, 2011.
- [19] A. M. dos Santos and E. A. Sousa, "Experimental treatment of the prototype of dc motor," *Research, Society and Development*, vol. 9, p. 91942848, 2020.
- [20] A. L. Nash, H. Pangborn, and N. Jain, "Robust control co-design with receding-horizon mpc," *2021 American Control Conference (ACC)*, pp. 373–379, 2021.
- [21] J. M. Bradley and E. Atkins, "Optimization and control of cyber-physical vehicle systems," *Sensors (Basel, Switzerland)*, vol. 15, pp. 23020 – 23049, 2015.
- [22] A. T. Al-Hammouri, M. S. Branicky, and V. Liberatore, "Co-simulation tools for networked control systems," in *Hybrid Systems: Computation and Control* (M. Egerstedt and B. Mishra, eds.), (Berlin, Heidelberg), pp. 16–29, Springer Berlin Heidelberg, 2008.
- [23] Q. Zhang, Y. Wu, L. Lu, and P. Qiao, "A single-loop framework for the reliability-based control co-design problem in the dynamic system," *Machines*, 2023.
- [24] A. Bhattacharya, S. Vasisht, V. Adetola, S. Huang, H. Sharma, and D. L. Vrabie, "Energy & buildings control co-design of commercial building chiller plant using bayesian optimization," *Energy & Buildings*, vol. 246, p. 111077, 2021.
- [25] T. Wati, Subiyanto, and Sutarno, "Simulation model of speed control dc motor using fractional order pid controller," *Journal of Physics: Conference Series*, vol. 1444, p. 012022, jan 2020.